The effects of soft and rough substrates on suction-based adhesion

Jonathan M. Huie[1,2,*], Adam P. Summers[2]

[1]Department of Biological Sciences, The George Washington University, Washington, DC 20052, USA

[2]Biology and SAFS, Friday Harbor Laboratories, University of Washington, Friday Harbor, WA 98250, USA

*Corresponding author: Jonathan M. Huie

Email: jonathanmhuie@gmail.com

Phone: +1 (669) 222-0582

Keywords: biomimetic, clingfish, modulus, overmolding, stress, work

SUMMARY STATEMENT

Clingfish and man-made suction cups adhere better on stiffer substrates than more compliant ones. Stiff cups can adhere to compliant rough surfaces, when they normally fail on hard rough ones.

ABSTRACT

The Northern clingfish (*Gobiesox maeandricus*) has a suction-based adhesive disc that can stick to incredibly rough surfaces, a challenge for stiff commercial suction cups. Both clingfish discs and bioinspired suction cups have stiff cores but flexible edges that can deform to overcome surface irregularities. Compliant surfaces are common in nature and technical settings, but performance data for fish and commercial cups is gathered from stiff surfaces. We quantified the interaction between substrate compliance, surface roughness, and suction performance for the Northern clingfish, commercial suction cups, and three biomimetic suction cups with disc rims of varying compliance. We found that all cups stick better on stiffer substrates and worse on more compliant ones, as indicated by peak stress values. On compliant substrates, surface roughness had little effect on adhesion, even for commercial cups that normally fail on hard, rough surfaces. We propose that suction performance on compliant substrates can be explained in part by effective elastic modulus, the combined elastic modulus from a cup-substrate interaction. Of all the tested cups, the biomimetic cups performed the best on compliant surfaces, highlighting their potential to be used in medical and marine geotechnical fields. Lastly, we discuss the overmolding technique used to generate the bioinspired cups and how it is an important tool for studying biology.

INTRODUCTION

Living systems have evolved diverse mechanisms for attachment in aquatic environments, including clamps, glues, hooks, and suction (Gorb 2008, Ditsche & Summers, 2014). Suction-based adhesion works on a variety of substrates and many fishes have independently evolved devices to generate suction. The clingfishes (Gobiesocidae), gobies (Gobiidae), lumpsuckers (Cyclopteridae), snailfishes (Liparidae), and shark suckers (Echeneidae) all have discs made from modified fin rays (Budney & Hall, 2010; Wainwright et al., 2013; Cohen et al., 2020, Palecek et al., 2021a; Woodruff et al., 2022). Balitorid loaches and suckermouth catfish use their whole bodies or fleshy lips, respectively, to adhere to substrates in freshwater streams (Lujan & Conway, 2015; Chuang et al., 2017; Bressman et al., 2020). The suctorial organ is used for more than station-holding, and in many cases it must resist the forces of locomotion or feeding. For example, freshwater gobies use suction to climb waterfalls (Blob et al., 2019; Palecek et al., 2021a). These waterborne biological suction cups are versatile devices, capable of adhering to different surfaces under diverse loading regimes.

The Northern clingfish (*Gobiesox maeandricus*) is a rocky intertidal specialist that uses its adhesive disc to resist high-energy waves and launch feeding attacks on attached limpets. Their disc works on the friable, rough, and low modulus surfaces that are a challenge for commercial suction cups. The Northern clingfish can produce attachment forces 80-250 times its body weight and adhere to incredibly rough surfaces, with grain sizes up to 1000 μm (Wainwright et al., 2013; Ditsche et al., 2014). On fouled surfaces covered in algae and biofilm, the fish is still able to produce adhesive forces up to 150 times its body weight (Ditsche et al., 2014). Clingfish discs are supported by modified bony elements from both the pectoral and pelvic girdles. On the contact surface, the fleshy disc margin is covered in a hierarchical array of microscopic papillae that match surface irregularities and facilitate adhesion on rough surfaces (Wainwright et al., 2013; Ditsche & Summers, 2019; Sandoval et al., 2020).

When challenged with sticking to stiff surfaces, commonly available commercial cups only work well on smooth surfaces, while biomimetic cups based on fish suckers also work well on rough surfaces (Ditsche & Summers, 2019; Sandoval et al. 2019). However, both the natural and technical world are filled with compliant surfaces such as fouled rocks in the intertidal or marine mammal skin (the target of tagging devices), and it is not clear how well current technology or natural technology (e.g., the clingfish suctorial disc) will adhere to a range of these surfaces. The mechanism behind high performance biomimetic cups on rough surfaces is that the edges of the disc deform to interlock with asperities on the surface. It is possible that a rough, compliant surface will deform to mimic a smooth surface and be tractable with commercial suction cups. Furthermore, a rough, compliant surface could deform to match the surface of a fish disc or a biomimetic cup more tightly, yielding an even higher performance (*i.e.*, potentially delaying cup failure and/or increasing adhesive loads). Alternatively, surfaces with a lower Young's modulus may be more difficult to adhere to and explain the loss in clingfish performance on fouled surfaces.

While substrate compliance may influence adhesive performance, the material properties of the suction cup is also likely to play an influential role. Soft single-material suction cups will adhere to rough surfaces by matching surface irregularities, but they peel prematurely leading to low attachment forces (Ditsche et al., 2016). Two-material suction cups, with a stiffer core and compliant edge, that replicate the clingfish's stiff supporting bones and its fleshy disc margin were effective on stiff, rough surfaces (Ditsche & Summers, 2019; Sandoval et al., 2019). A potentially fertile ground for technical innovation is learning whether two part biomimetic cups have high performance on compliant and rough surfaces. The two-material design also provides the foundations for a plethora of potential biomimetic cups that vary in the stiffness of their core and disc rim, some of which may be better suited for specific roles in the human health arena (*e.g.,* transporting fragile organs) and the marine geotechnics field (*e.g.,* building machines with suction-based grabbers or suction-based climbing robots) (Yoshida and Ma, 2010; Sandoval et al., 2019; Martinez et al. 2021). Therefore, devising a relatively simple and cost-effective method for generating biomimetic cups is of broader interest.

There is no obvious theoretical framework for predicting how suction cups of varying compliance will perform on surfaces of varying compliance and roughness. Two likely important factors are 1) the combined stiffness of the two materials, and 2) the interaction between roughness and stiffness. For the first issue we can look to the field of contact mechanics, which quantifies area of contact for objects pressed into one another. The shape, and the force pushing the two objects into contact are important, and so is the notion of effective elastic modulus – the combined elastic moduli of the two objects. Effective elastic modulus appears in a solution to the problem of two spheres in contact and neatly accounts for the fact that when two objects of different stiffness come in contact it does not matter which is compliant and which is stiff, just that one or the other is (Hertz, 1881). Contact area, which is a predictor of adhesive force, is also dependent on roughness. The rougher a material the smaller the effective contact area is with respect to the measured contact area.

In this study, we investigated the interactions between substrate compliance, cup compliance, and surface texture. We had three specific aims: 1) develop a method for quickly and inexpensively fabricating two material, biomimetic suction cups; 2) quantify the interaction between substrate compliance and suction-based adhesion; and 3) determine the effect of surface roughness in the context of varying compliance, on suction performance. By answering these questions, we will better our understanding of both the technical solutions to suction and the implications of substrate properties on suction for fishes.

MATERIALS AND METHODS

Seventeen Northern clingfish (*Gobiesox maeandricus*) were collected in the intertidal of San Juan Island, Washington, USA near Friday Harbor Laboratories. Live animals were housed in a flow-through system prior to adhesion testing. Shortly before testing, specimens were euthanized with MS-222, weighed, and photographed to measure standard length and disc area (Figure 1A). The animals ranged from 5.6 to 11.7 cm in standard length, from 3.5 to 30.8 g in mass, and had adhesive discs that varied between 2.1 and 12.3 cm^2 in area (see supplemental material for all fish measurements). This research was conducted under an IACUC protocol from the University of Washington at the Friday Harbor Laboratories.

Surface and suction cup generation

We created ten substrates to test the interaction of substrate stiffness and surface roughness on adhesion. Three variants of a platinum-catalyzed silicone rubber were used to vary substrate compliance (Smooth-On Inc., Ecoflex™ Series; 00-10, 00-30, and 00-50, each with a maximum tensile strength of 0.8 MPa, 1.4 MPa, and 2.1 MPa, and a Young's modulus at 100% elongation of 55 kPa, 69 kPa, and 83 kPa as reported by the manufacturer). We selected these materials because the stiffness range spans that of fouled marine surfaces (Ditsche & Summers, 2019). We could not get stiffer material with the same formulation, and would have to add an effect of polymer chemistry if we moved to a stiffer urethane. We used a mold to generate the substrates for each silicone variant. To incorporate surface roughness, we cast the substrates directly onto a sheet of glass or one of two kinds of sandpaper (Buehler CarbiMet™ 2; P60 and P240, matching average grit sizes of 59 and 269 μm, respectively). The silicones were prepared by mixing equal quantities of the Part A and Part B rubbers as instructed by the manufacturer. The casts were allowed to cure at room temperature for at least 24 h and then glued to the base of watertight plastic containers. The tenth substrate was made using epoxy resin to act as a smooth, hard surface.

In addition to clingfish, we also tested the adhesion of man-made suction cups. First, a readily available and commercially sold polyvinyl chloride suction cup (Adams Manufacturing Corp.; 6.42 cm^2 in area), hereafter referred to as the 'commercial' cup (Figure 1B). To test the interaction between cup compliance and substrate compliance on adhesion, we created three kinds of two-material biomimetic cups by overmolding silicone onto the commercial suction cups (all cups were 10.35 cm^2 in area) inspired by Ditsche and Summers (2019) (Figure 1C). We made these three overmold variants using the same three Ecoflex silicones we used for the substrates. The overmolding procedure involved a two-part 3D printed mold, where the commercial cup sat in the cavity of the mold that was later filled with silicone rubber (see Figure 1D for a schematic of the overmolding design). Cyanoacrylate glue was used to ensure the edges of the silicone overmold were firmly attached to the commercial cup. We tested three replicates of the commercial cup and each overmold cup variant.

Measuring suction performance

We measured the maximum adhesive force of freshly euthanized clingfishes and the man-made suction cups with a MTS Synergie 100 materials testing machine (see Figure 1E for a schematic of the set up). Adhesive, or 'suction', force was considered to be the amount of force required to pull a specimen off a given substrate. To attach the clingfish to the MTS, we threaded fishing line through the body creating a harness of three loops above and around the disc. A separate line was threaded through the harness and hooked onto the moving cross head of the MTS. For the man-made cups, we tied two loops to the top of the cups and threaded a line through the loops that attached to the crosshead of the MTS. The substrate containers were mounted on to the base of the MTS and filled with just enough seawater to cover the specimens.

Prior to each test, we gently pressed the fish or cup against the substrate to evacuate water from underneath the cup and ensure adhesion. Each fish was preconditioned with three tests that were discarded and then tested on all nine substrates in a random order. Five trials were recorded consecutively for each specimen-substrate pair before changing substrates. To generate data comparable to that of previous studies, all tests were conducted with the crosshead moving at a constant speed of 1 m min^{-1} and force continually recorded at 500 Hz. Only the man-made suction cups were tested on the hard epoxy substrate. However, we obtained published force data that was collected in a similar manner for the Northern clingfish (n = 32) on smooth, hard epoxy surfaces (Wainwright et al., 2013; Ditsche & Summers, 2019) .

Only the maximum force measurements from each specimen-substrate pair were used in subsequent analyses. To account for the effect of cup size on attachment force, we calculated tensile stress (P_{ad}) as a function of the measured attachment force (F_{ad}) over the surface area of the suction disc (A) as follows:

$$P_{ad} = \frac{F_{ad}}{A} \qquad (1)$$

Peak attachment forces were determined using the load extension curves. For each trial, we set zero extension point to be where the load increased 0.1 N over a baseline. The baseline was calculated by averaging 15 points gathered before slack was taken up on the attachment string. Peak attachment force was considered the highest recorded load prior to cup detachment, marked by a sudden drop in load. When adhesion is due to suction and we ignore the cohesion of water, the maximum tensile stress of any suction cup at sea level and standard atmospheric pressure is theoretically 101 kPa. However, Smith (1991) used artificial seawater to empirically derive a maximum stress of 168 kPa. While water has great cohesion, this is undermined in practice by microbubbles and impurities that provide nucleation sites for an expanding gas bubble. The theoretical and empirically derived maximums provide context for the performance of our tested suction cups.

To better understand the effects of different substrates on suction cup performance, we also calculated the amount of time until each cup detached from the surface and the amount of work required to remove them. Attachment time was calculated as the total time between the zero extension point and sudden drop in load. The amount of work required to remove each cup from the substrate was measured as the area under the load-extension curve. Work differs from peak stress because stress is determined solely by force and work is the energy needed to detach a cup. It is important to make this distinction because our testing method ramped up the force from zero at a regular, and relatively slow, rate determined by extension. But, in a biologically, or technically relevant scenario the load might be applied very rapidly and removed with equal rapidity. It could be that peak force really does determine attachment failure in this scenario, but it is more likely that the energy applied to the system determines failure. A very large transient force may not dislodge a cup, but a sub-peak force applied over a long time will. So, we assessed both peak stress and work because of the potential that real world applications will be quite different from our testing set up. For the clingfish, we were unable to calculate time or work on the smooth, hard epoxy surface.

Statistical Analyses

We performed linear mixed-effect models to compare the effects of substrate compliance and surface roughness on peak stress, work, and time. With a mixed-effect framework, we placed greater emphasis on comparing how much effect sizes differed instead of calculating p-values, partially because we had relatively low sample sizes for the man-made cups. For each of the five suction cup types (clingfish, commercial, and the three overmolded cups), we performed three models, one for each variable using the *lme4* R package (Bates et al., 2015). All models followed a similar structure with substrate compliance and surface roughness (and their interaction) included as fixed effects, and individual fish or cup number as a random effect to account for repeated measures (y ~ Substrate Stiffness * Surface Roughness + (1|Individual)). To summarize the fixed effects and calculate the mean values, standard errors, and confidence intervals on each substrate, we used the *eemeans* R package (Lenth, 2019). The coefficient of determination or goodness-of-fit of each model was calculated as Nagakawa's marginal R^2 ($R^2_{LMM(m)}$, which describes the amount of variation explained by only the fixed effects) and conditional R^2 ($R^2_{LMM(c)}$; which describes the amount of variation explained by both the fixed and random effects), using the *performance* R package (Lüdecke et al., 2019). All statistical analyses were performed in R version 4.0.2 (R Core Team, 2020).

Effective elastic modulus

Lastly, we assessed whether peak stress correlated with the effective elastic modulus of the suction cup and substrate. If we consider that contact area is an important component of peak stress, then it makes sense to look to contact theory for a parameter to describe the interaction between the stiffness of the two bodies. Hertzian contact theory, and Johnson-Kendall-Roberts contact theory (the modern modification that considers adhesive contact) have a parameter called effective elastic modulus, that accounts for two materials (Hertz, 1881, Johnson et al., 1971). The formula for the inverse of effective elastic modulus is the sum of the inverses of the two moduli scaled by their Poisson's ratio, and is similar in form to the Rule of Mixtures used in determining the effective modulus of a composite. In that case, rather than Poisson's ratio, the modulus is scaled by the relative volume of each material in the composite (Alger, 1996; Liu et al., 2009). Effective elastic modulus (E_{ff}) describes the overall elastic deformation of two contacting surfaces and was calculated as:

$$E_{ff} = \left(\frac{(1 - v_1^2)}{E_1} + \frac{(1 - v_2^2)}{E_2}\right)^{-1} \quad (2)$$

where E_1 and v_1, and E_2 and v_2 represent the elastic moduli and Poisson's ratio of the suction cup and substrate, respectively. For the overmolded suction cups, we used the 100% modulus of the Ecoflex (as reported by the manufacturer) used to make the disc rim and assumed a Poisson's ratio of 0.5, which is typical of more compliant elastomers. We fit three linear models of increasing complexity to describe the relationship between the inverse of effective elastic modulus and peak stress. We used the inverse of effective elastic modulus instead of E_{ff} because the calculated values spanned several orders of magnitude and did not appear to exhibit a linear relationship with stress (see Results). These models fit, 1) a single line through all of the data points, 2) one line through the commercial cups and another through all of the overmold cups, and 3) one line through the commercial cups and a separate line through each of the three overmold cups. The model with the lowest AIC (Akaike's Information Criterion) score was used to describe the data.

RESULTS

Effects of surface stiffness and roughness on tensile stress

All suction cups (clingfish and man-made) generally adhered better on the stiffest substrates and worst on the most compliant ones (Figure 2; Table 1). Meanwhile, surface roughness and its interaction term with substrate stiffness had only a small effect on peak stress, indicated by the overlapping means and confidence intervals (Table 1). While the stress of commercial suction cups on smooth epoxy (86.6 ± 1.44 kPa) approached the theoretical adhesive maximum in air (101 kPa), no cups exceeded it or came close to the empirical maximum of 168 kPa in seawater. Most cups performed between 1/4 and 1/2 of the theoretical maximum and between 1/5 and 1/3 of the empirical maximum.

Overall, the clingfish performed the worst of the five cups. On the stiffest silicone substrate (Ecoflex 50), clingfish adhesive forces varied between 108 and 261 times their body weight and peak stress varied between 27.1 and 45.1 kPa (mean = 33.4 ± 1.44 kPa), which was on average 62% better than when on the most compliant Ecoflex 10 substrate. For the clingfish, there was no difference in peak stress on the stiffest silicone substrates and the hard epoxy, (Figure 2; Table 1). Meanwhile, the commercial cups peak stress values on the hard epoxy ranged between 84.8 and 89.2 kPa (mean = 86.6 ± 1.44 kPa), which were on average 65% higher than on the stiffest silicone substrates and 260% higher than on the most compliant substrates. The different overmold suction cups all had similar stress values so here we report their results in aggregate, but full details are presented in Table 1. Their peak stress on the hard epoxy substrate ranged between 50.2 and 56.0 kPa (mean = 53.5 ± 0.691 kPa), which was on average 15% higher than on the stiffest silicone substrate and 68% higher than when on the most compliant substrate. In sum, the commercial cups outperformed the clingfish and overmold cups on the two stiffest substrates, the overmold cups performed better than the clingfish and commercial cups on the more compliant substrates.

Effects of surface stiffness and roughness on time and work

Larger clingfish took longer to be detached than smaller individuals, but all clingfish generally remained attached for longer on the more compliant substrates. On the Ecoflex 10 substrates, they were attached for 0.959 ± 0.030 s before being dislodged, which was 20% longer than on the Ecoflex 50 substrates (Figure 3; Table 2). By contrast, the commercial cups adhered for longer on stiffer substrates. On the hard epoxy they remained attached for 1.147 ± 0.148 s, which was 60% longer than on the most compliant substrates (Figure 3; Table 2). The overmold cups did not show any clear trends and also differed between cups (Figure 3; Table 2). The overmold cups with the Ecoflex 10 and Ecoflex 50 disc rims both showed no effect of substrate compliance and attachment time on the silicone substrates. The Ecoflex 10 cups remained attached for 1.075 ± 0.050 s on all silicone substrates, while the Ecoflex 50 cups did slightly better 1.353 ± 0.058 s. On the hard epoxy, both cup types remained attached 50% longer than they did on the compliant substrates, while the Ecoflex 30 cups remained adhered for the same amount of time across all substrates (1.167 ± 0.042 s) (Figure 3; Table 2).

The man-made suction cups required more work to be detached from stiffer substrates and less on the more compliant ones (Figure 4; Table 3). Clingfish required equal amounts of work to be removed from all substrates, with larger individuals generally requiring more work than smaller ones (0.066 ± 0.003 mJ) (Figure 4; Table 3). The commercial cups required an average of 0.436 ± 0.057 mJ of work to be removed from the epoxy substrate, which was nearly 4 times more work than on the most compliant silicone substrate. All three overmold cups showed similar work values, in that they required 0.575 ± 0.034 mJ of work to be removed from the epoxy surface and half of that amount on the most compliant silicone substrates. Surface roughness and the interaction with substrate stiffness had little to no effect on time or work (Figures 3; 4; Tables 2; 3).

Effective elastic modulus and tensile stress

For man-made suction cups on smooth and rough surfaces, peak stress increased with effective elastic modulus (E_{ff}) in a nonlinear fashion (Figure 5A). Instead, our data suggest that the relationship is more asymptotic, where peak stress increases with effective elastic modulus to an extent and eventually levels off. By contrast, peak stress was negatively correlated with the inverse of effective elastic modulus (Figure 5B). The data were best described with the most complex model that fit a separate line for the commercial cups and each of the three overmold cups, which explained 86.4% of the variation (adjusted $R^2 = 0.864$, F-statistic = 109.1, df = 112, p-value < 0.001, AIC = 699.7). The relationship between peak stress and the inverse of effective elastic modulus (as well as the untransformed modulus) varied relatively little among overmold cups, but the relationship between the commercial cup and the overmold cup differed greatly (Figure 5). The equation for the commercial cup regression line was $P_{ad} = -4832.88 * E_{ff} + 90.23$. Meanwhile, regression line for the overmold suction cups with the Ecoflex 10 disc rim was $P_{ad} = -2039.46 * E_{ff} + 88.16$, for the Ecoflex 30 disc rim it was $P_{ad} = -1533.48 * E_{ff} + 72.76$, and for the Ecoflex 50 disc rim it was $P_{ad} = -1533.74 * E_{ff} + 71.13$. The two less complex models also explained a large portion of the variation. The model that fit a common line through all of the overmold cups explained 83.7% of the variation (adjusted $R^2 = 0.837$, F-statistic = 204.4, df = 116, p-value < 0.001, AIC = 717.9), and a common line through all of the man-made cups explained 26.0% of the variation (adjusted $R^2 = 0.260$, F-statistic = 42.74, df = 118, p-value < 0.001, AIC = 897.4).

DISCUSSION

Stiff commercially available suction cups simply will not stick to hard, rough surfaces – that requires a compliant cup. Biomimetic cups with flexible disc rims do better on stiff, rough surfaces than the clingfish they are modeled on (biomimetic cup stress: 55–61 kPa; clingfish stress: 28–55 kPa) (Wainwright et al., 2013; Ditsche & Summers, 2019). Thus, our findings that commercial cups equally adhere well to the rough silicone substrates (stress: 20–56 kPa) provide insight on the factors that contribute to successful adhesion. Either the cup or the substrate needs to be compliant if the surface is rough, and that different degrees of roughness have little effect on performance when the substrate is compliant. However, there is a substantial penalty for substrate compliance. For all suction cups on the most compliant substrates, peak suction is around 25% of the theoretical maximum of 101 kPa in air and 20% of an empirical maximum of 168 kPa derived in seawater (Smith, 1991) and is substantially worse than on stiffer substrates. What we take away from this is two fold.

First, there is an interaction between the surface and the cup that can be quantified with effective elastic modulus. This point makes intuitive sense when considering the way stiff cups fail on hard, rough surfaces. Because they do not comply with the rugosities of the surface, there is leakage under the disk and suction is never established. A compliant cup conforms to the surface asperities and allows negative pressure. In the same vein, if the cup is stiff and the surface is rough but compliant, the surface asperities will deform and allow the hard cup to generate suction. However, knowing this implies that there is a threshold, or a maximum elastic modulus that a rough surface can have before a hard cup will no longer be able to stick to it. There also appears to be a limit on how much the effective elastic modulus of a cup-substrate system can be increased to optimize adhesion. More data on other cups and surfaces that encompass a wider range of material properties are needed to find the threshold and to buttress the relationship between effective elastic modulus and peak stress.

The second takeaway is that it is very difficult to stick to compliant surfaces, which might explain why the peak stress of the Northern clingfish suffers on fouled surfaces (Ditsche et al., 2014). However, all man-made suction cups outperformed the clingfish on the compliant silicone substrates. These discrepancies may be explained by any number of design differences from the symmetry to the simplicity of the man-made cups. Our method of testing the suction cups, by applying tension at a constant rate in only the dorsal-ventral direction, may also be a poor representation of the hydrodynamic forces the Northern clingfish have evolved to withstand. Furthermore, there is little reason for the Northern clingfish to excel on compliant substrates since they are found on hard rocky surfaces. Unlike commercial cups which are optimized for performance and cost by consumer demand, evolutionary selective pressures act only to make the clingfish adhesive disc good enough rather than optimal (Martinez et al., 2021). Additionally, the clingfish required equal amounts of work to be detached from all of the compliant substrates, suggesting that in nature, where clingfish often stick to fouled surfaces, there is effectively no loss in performance. Nevertheless, it may be worth investigating the performance of specialist clingfish species with a distinct double-cup design that spend most of their time sticking to compliant surfaces like seagrass and macroalgae (Conway et al., 2019; Conway et al., 2020).

Our findings that biomimetic suction cups can stick to our most challenging surfaces is exciting because grabbing onto rough and compliant substrates is a challenge. Mechanical grippers may exceed the strength of material and leave permanent damage. We show that commercial suction cups could work, but peak stress will be low. Biomimetic cups had higher stress and work on compliant substrates than hard commercial cups regardless of surface texture, and the difference between the cups went up as the elastic modulus of the substrate decreased (up to a ~30% difference in stress on the most compliant substrate). In other words, biomimetic cups perform better on trickier substrates, and the more difficult the substrate the more effective the biomimetic cups were relative to the commercially available version. Stiffer overmold cups also remained attached to compliant surfaces for longer, without increasing their suction forces. Disc rim compliance and the relationship between effective elastic modulus and peak stress are design imperatives that will drive the invention of specialized biomimetic cups that maximize suction and adhesion time on targeted substrates. For example, in the medical field, biomimetic cups could be used to pick up and retract or transport delicate internal organs. Suction can also be the attachment method for non-invasive tags on free living marine mammals, which have a soft outer layer of skin and blubber (Grear et al., 2018; Ditsche & Summers, 2019); they could be attached to the arms of underwater vehicles for handling and retrieving delicate objects (Sandoval et al., 2019); or they could allow suction-based robots to traverse challenging surfaces (Yoshida and Ma, 2010).

Overmolding is both an important and underutilized technique for biological investigations from the imitation of attachment devices to the exploration of skeletal function. Overmolding is commonly used in manufacturing but is rarely applied to biology. The procedure we used requires relatively low cost, commercially available materials, making it broadly accessible. Overmolding techniques can be extended to variable soft tissue morphologies found in other fish adhesive discs to improve biomimetic cups. Furthermore, 3D printed biomimetic skeletal models, or canonical support structures, can be embedded into flexible silicone rubber to explain the functional implications of the structure of the stiff core. An overmolding procedure similar to ours did exactly this to study how pelvic girdle shape influences suction performance in fishes with adhesive discs (Palecek et al., 2021b). Beyond suction cups, overmolding could be used to model the wing-like fins of batoids and be combined with multi-material 3D printing to mimic materially complex biologies in much greater detail (Schaefer & Summers, 2005, Frølich et al., 2017; Bader et al., 2018). Overmolding is a widely applicable and adjustable technique that should be used in future bio-inspired studies.

ACKNOWLEDGMENTS

We thank Sandy Kawano for providing advice about mixed-effect models. We thank Petra Ditsche for insightful discussion and Amanda Palacek-McClung for reviewing an early draft of the manuscript. Karly Cohen was key to accessing some of our data in the confines of a pandemic stressed world.

COMPETING INTERESTS

The authors declare no competing interests.

AUTHORS' CONTRIBUTIONS

JMH designed the study, collected the data, performed statistical analyses, and wrote the manuscript. APS conceived the study, designed the study, and wrote the manuscript. Both authors gave their final approval for publication.

FUNDING

APS and JMH were supported by the Seaver Institute and the National Science Foundation (DEB-1701665 and DBI-1759637; DGE-1746914 to JMH).

DATA AVAILABILITY

All datasets and corresponding R code used in this study are provided in the supplemental materials.

REFERENCES

Alger, M. (1996). *Polymer science dictionary*. Springer Science & Business Media.

Bader, C., Kolb, D., Weaver, J.C., Sharma, S., Hosny, A., Costa, J., and Oxman, N. (2018). Making data matter: Voxel printing for the digital fabrication of data across scales and domains. *Sci. Adv.* **4**, eaas8652. (doi:10.1126/sciadv.aas8652)

Bates, D., Maechler, M., Bolker, B., and Walker, S. (2015). Fitting linear mixed-effects models using lme4. *J. Stat. Softw*. **67**, 1–48. (https://doi.org/doi:10.18637/jss.v067.i01)

Blob, R.W., Lagarde, R., Diamond, K.M., Keeffe, R.M., Bertram, R.S., Ponton, D., and Schoenfuss, H.L. (2019). Functional Diversity of Evolutionary Novelties: Insights from Waterfall-Climbing Kinematics and Performance of Juvenile Gobiid Fishes. *Integr. Org. Biol.* **1**, obz029. (doi:10.1093/iob/obz029)

Budney, L.A and Hall, B.K. (2010). Comparative morphology and osteology of pelvic fin-derived midline suckers in lumpfishes, snailfishes and gobies. *J. Appl. Ichthyol.* **26**, 167–175. (doi:10.1111/j.1439-0426.2010.01398.x)

Bressman, N.R., Armbruster, J.W., Lujan, N.K., Udoh, I., and Ashley-Ross, M.A. (2020). Evolutionary optimization of an anatomical suction cup: Lip collagen content and its correlation with flow and substrate in Neotropical suckermouth catfishes (Loricarioidei). *J. Morphol.* **281**, 676–687. (doi:10.1002/jmor.21136)

Chuang, Y.C., Chang, H.K., Liu, G.L., and Chen, P.Y. (2017). Climbing upstream: Multi-scale structural characterization and underwater adhesion of the Pulin river loach (*Sinogastromyzon puliensis*). *J. Mech. Behav. Biomed. Mater.* **73**, 76–85. (doi:10.1016/j.jmbbm.2017.01.029)

Cohen, K.E., Crawford, C.H., Hernandez, L.P., Beckert, M., Nadler, J.H., and Flammang, B.E. (2020). Sucker with a fat lip: The soft tissues underlying the viscoelastic grip of remora adhesion. *J. Anat.* **237**, 643–654. (doi:10.1111/joa.13227)

Conway, K.W., Moore, G.I., and Summers, A.P. (2019). A new genus and two new species of miniature clingfishes from temperate southern Australia (Teleostei, Gobiesocidae). *ZooKeys* **864**, 35. (doi: 10.3897/zookeys.864.34521)

Conway, K.W., King, C.D., Summers, A.P., Kim, D., Hastings, P.A., Moore, G.I., Iglésias, S.P., Erdmann, M.V., Baldwin, C.C., Short, G., and Fujiwara, K. (2020). Molecular phylogenetics of the clingfishes (Teleostei: Gobiesocidae)—implications for classification. *Copeia* **108**, 886-906. (doi: 10.1643/CI2020054)

Ditsche, P. and Summers A.P. (2014). Aquatic versus terrestrial attachment: Water makes a difference. *Beilstein J. Nanotechnol.* **5**, 2424–2439. (doi:10.3762/bjnano.5.252)

Ditsche, P., Wainwright, D.K., and Summers, A.P. (2014). Attachment to challenging substrates - Fouling, roughness and limits of adhesion in the northern clingfish (*Gobiesox maeandricus*). *J. Exp. Biol.* **217**, 2548–2554. (doi:10.1242/jeb.100149)

Ditsche, P., Ford, W., and Summers, A.P. (2016). The role of cup elasticity in suction attachment in Northern Clingfish. In *Society for Integrative and Comparative Biology Annual Meeting, 3–7 January, Portland, OR.* (www.sicb.org/meeting/2016/SICBOral.pdf)

Ditsche, P. and Summers, A.P. (2019). Learning from Northern clingfish (*Gobiesox maeandricus*): Bioinspired suction cups attach to rough surfaces. *Philos. Trans. R. Soc. B Biol. Sci.* **374**, 20190204. (doi:10.1098/rstb.2019.0204)

Frølich, S., Weaver, J.C., Dean, M.N., and Birkedal, H. (2017). Uncovering Nature's Design Strategies through Parametric Modeling, Multi-Material 3D Printing, and Mechanical Testing. *Adv. Eng. Mater.* **19**, e201600848. (doi:10.1002/adem.201600848)

Gorb, S.N. (2008). Biological attachment devices: Exploring nature's diversity for biomimetics. *Philos. Trans. R. Soc. A Math. Phys. Eng. Sci.* **366**, 1557–1574. (doi:10.1098/rsta.2007.2172)

Grear, M.E., Motley, M.R., Crofts, S.B., Witt, A.E., Summers, A.P., and Ditsche, P. (2018). Mechanical properties of harbor seal skin and blubber − a test of anisotropy. *Zoology* **126**, 137–144. (doi:10.1016/j.zool.2017.11.002)

Hertz, H. (1881). On the contact of elastic solids. *Z. Reine Angew. Mathematik*, *92*, pp.156-171.

Huie, J.M. and Summers, A.P. (2022). Measuring clingfish pull-off forces. Figshare. (doi:10.6084/m9.figshare.19586668.v2)

Johnson, K.L., Kendall, K., and Roberts, A.D. (1971). Surface energy and the contact of elastic solids. *Proc. R. Soc. London. A. Math. Phys. Sci.* **324**, 301–313. (doi:10.1098/rspa.1971.0141)

Lujan, N.K. and Conway, K.W. (2015). Life in the fast lane: a review of rheophily in freshwater fishes. In *Extremophile Fishes: Ecology, Evolution, and Physiology of Teleosts in Extreme Environments* (eds R Riesch, M Tobler, M Plath), pp. 107–136. Cham: Springer International Publishing. (doi: 10.1007/978-3-319-13362-1_6)

Lenth, R. (2019). emmeans: estimated marginal means, aka least-squares means. R package version 1.4.3. https://CRAN.R-project.org/package=emmeans.

Liu, B., Feng, X., and Zhang, S.M. (2009). The effective Young's modulus of composites beyond the Voigt estimation due to the Poisson effect. *Compos. Sci. and Technol.* **69**, 2198-2204 (doi: 10.1016/j.compscitech.2009.06.004).

Lüdecke, D., Makowski, D., and Waggoner, P. (2019) performance: assessment of regression models performance. R package version 0.4.0. https://CRAN.Rproject.org/package=performance.

Martinez, A., DeJong, J., Akin, I., Aleali, A., Arson, C., Atkinson, J., Bandini, P. Baser, T., Borelai, R., Boulanger, R., *et al.* (2021). Bio-inspired geotechnical engineering: Principles, current work, opportunities and challenges. *Géotechnique,* 1–48. (doi: 10.1680/jgeot.20.P.170)

Palecek, A.M., Schoenfuss, H.L., and Blob, R.W. (2021a). Sticking to it: testing passive pull-off forces in waterfall-climbing fishes across challenging substrates. *J. Exp. Biol.* **224**. (doi: 10.1242/jeb.228718)

Palecek, A.M., Huie, J.M., Cohen, K.E., Donatelli, C.M., and Summers, A.P. (2021b). Stuck on you: How pelvic girdle morphology influences adhesion. In *Society for Integrative and Comparative Biology Virtual Annual Meeting, 3 January–28 February*. (https://sicb.burkclients.com/meetings/2021/schedule/abstractdetails.php?id=259)

R Core Team. 2017 R: A language and environment for statistical computing. R Foundation for Statistical Computing, Vienna, Austria. (https://www.R-project.org/)

Sandoval, J.A., Jadhav, S., Quan, H., Deheyn, D.D., and Tolley, M.T. (2019). Reversible adhesion to rough surfaces both in and out of water, inspired by the clingfish suction disc. *Bioinspiration and Biomimetics* **14**, 66016. (doi:10.1088/1748-3190/ab47d1)

Sandoval, J.A., Sommers, J., Peddireddy, K.R., Robertson-Anderson, R.M., Tolley, M.T., and Deheyn, D.D. (2020). Toward Bioinspired Wet Adhesives: Lessons from Assessing Surface Structures of the Suction Disc of Intertidal Clingfish. *ACS Appl. Mater. Interfaces* **12**, 45460–45475. (doi:10.1021/acsami.0c10749)

Schaefer, J.T. and Summers, A.P. (2005). Batoid wing skeletal structure: Novel morphologies, mechanical implications, and phylogenetic patterns. *J. Morphol.* **264**, 298–313. (doi:10.1002/jmor.10331)

Schindelin, J., Arganda-Carreras, I., Frise, E., Kaynig, V., Longair, M., Pietzsch, T., Preibisch, S., Rueden, C., Saalfeld, S., Schmid, *et al*. (2012). Fiji: an open-source platform for biological-image analysis. *Nat. Methods* **9**, 676–682. (doi: https://doi.org/10.1038/nmeth.2019)

Wainwright, D.K., Kleinteich, T., Kleinteich, A., Gorb, S.N., and Summers, A.P. (2013). Stick tight: Suction adhesion on irregular surfaces in the northern clingfish. *Biol. Lett.* **9**, 20130234. (doi:10.1098/rsbl.2013.0234)

Woodruff, E.C., Huie, J.M., Summers, A.P., and Cohen, K.E. (2022). Pacific Spiny Lumpsucker armor—Development, damage, and defense in the intertidal. *J. Morphol.* **283**, 164–173. (doi.org/10.1002/jmor.21435)

Yoshida, Y., and Ma, S. (2010). Design of a wall-climbing robot with passive suction cups. In *2010 IEEE International Conference on Robotics and Biomimetics*. pp. 1513-1518.

Figures and Tables

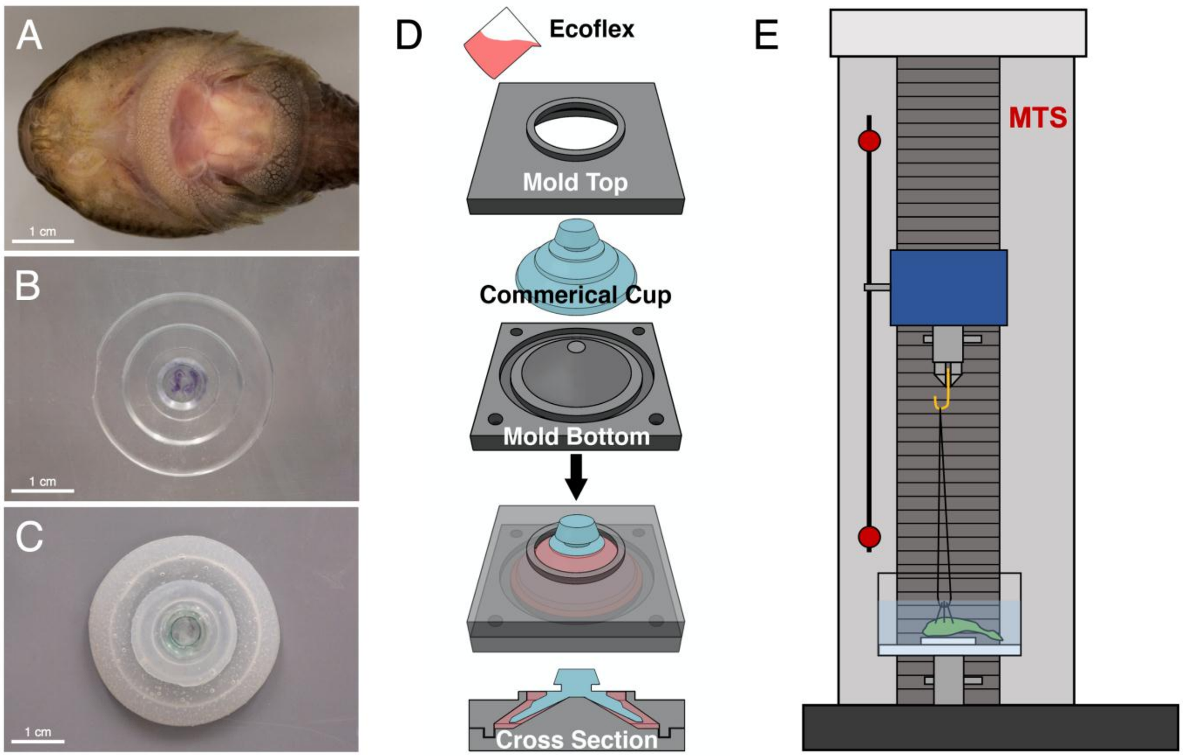

Figure 1. Examples of the three types of cups tested in this study A) the Northern clingfish, B) a commercial suction cup, and C) an overmolded commercial cup. Schematic D) represents the overmolding procedure used to add a silicone disc rim to the commercial cups. Our test set up to measure the pull-off forces of each cup is depicted in E), including the harness used to attach the clingfish to the moving crosshead of the materials testing machine (drawing from Huie & Summers, 2022).

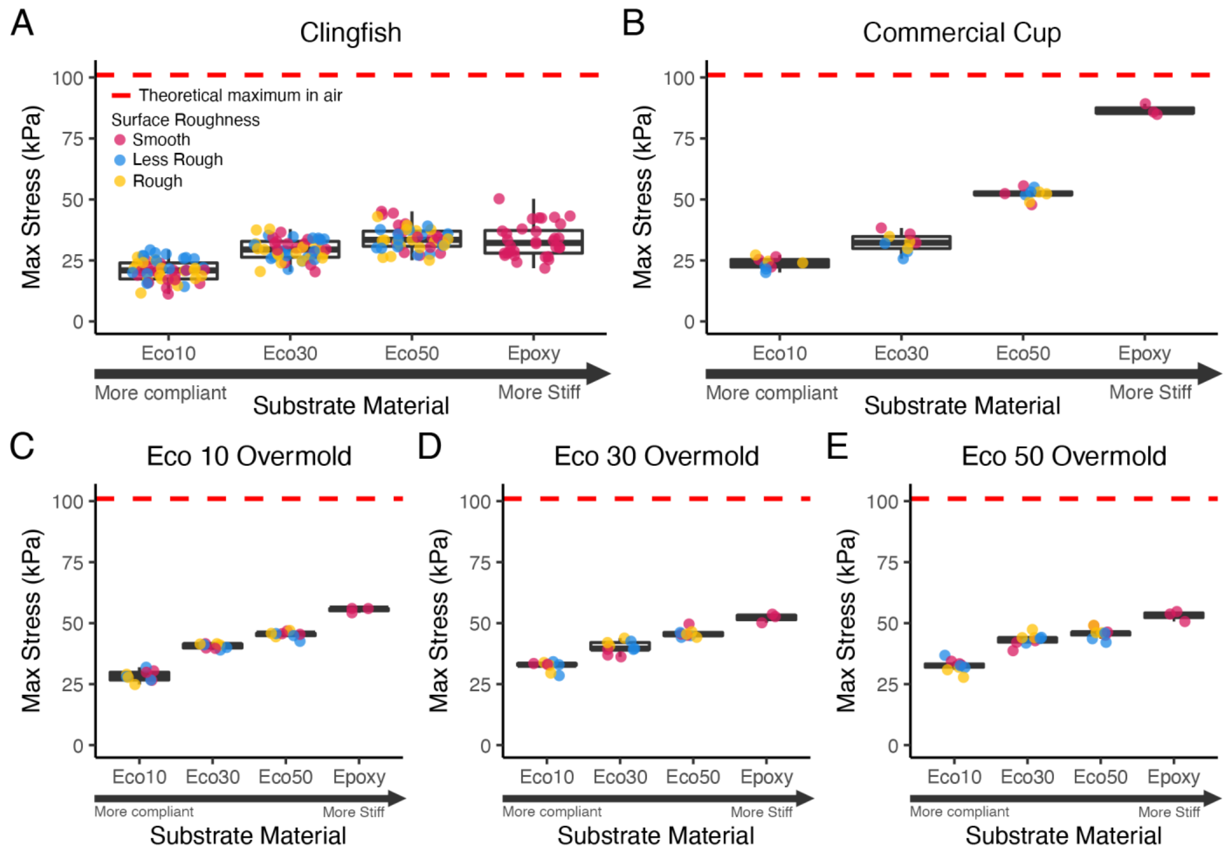

Figure 2. Maximum tensile stress (kPa) for A) the Northern clingfish, B) commercial suction cups, and C-D) the different overmold suction cups on substrates of varying compliance and surface roughness. Boxplots show the median, upper and lower quartiles, and interquartile range. Dots are individual observations colored by the surface roughness (Magenta = Smooth (0 µm), Blue = Less Rough (59 µm), and Yellow = Rough (269 µm)), to indicate that surface roughness had little or no effect on max stress for any cup type. Red dotted line indicates the theoretical adhesive maximum when in air (101 kPa). No cups approached the empirical maximum derived in seawater at sea level (168 kPa).

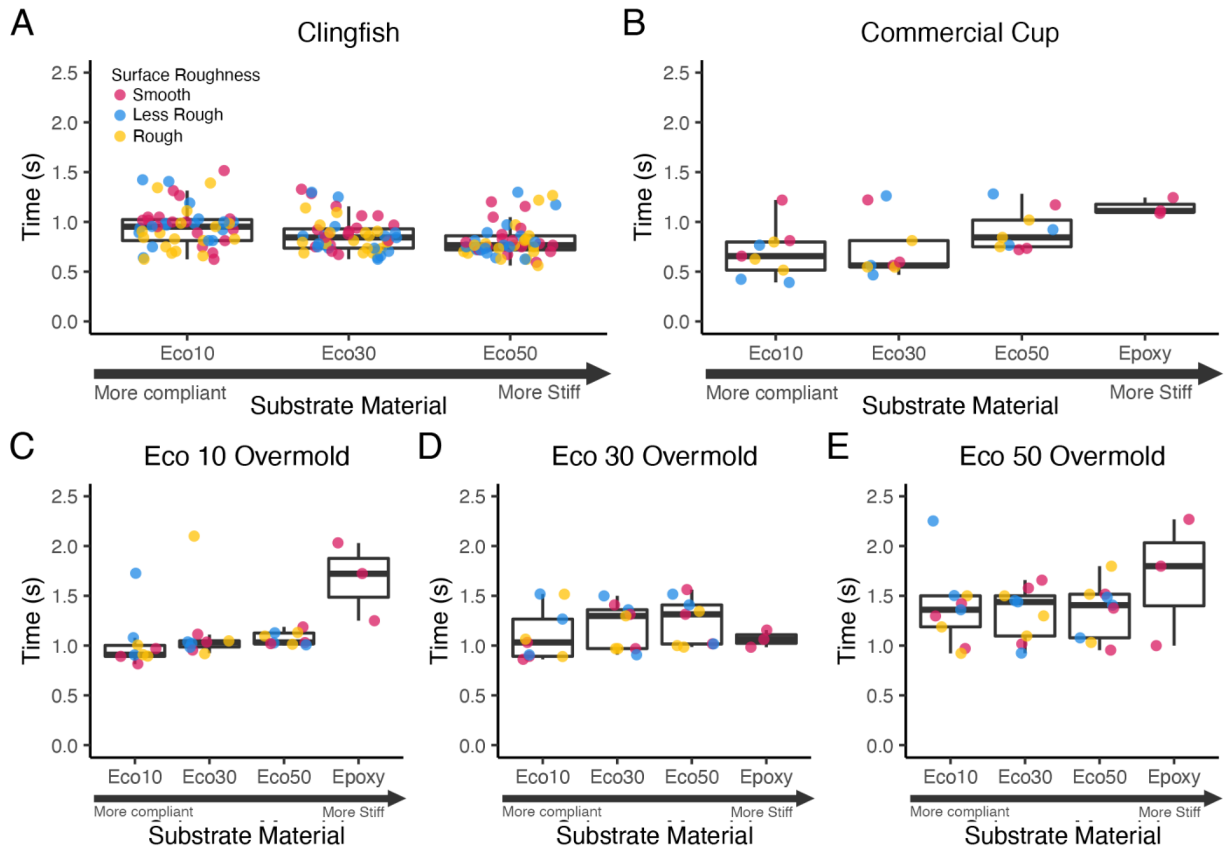

Figure 3. The amount of time (s) until detachment for A) the Northern clingfish, B) commercial suction cups, and C-D) the different overmold suction cups from substrates of varying compliance and surface roughness. Boxplots show the median, upper and lower quartiles, and interquartile range. Dots are individual observations colored by the surface roughness (Magenta = Smooth (0 µm), Blue = Less Rough (59 µm), and Yellow = Rough (269 µm)), to indicate that surface roughness had little or no effect on max time for any cup type.

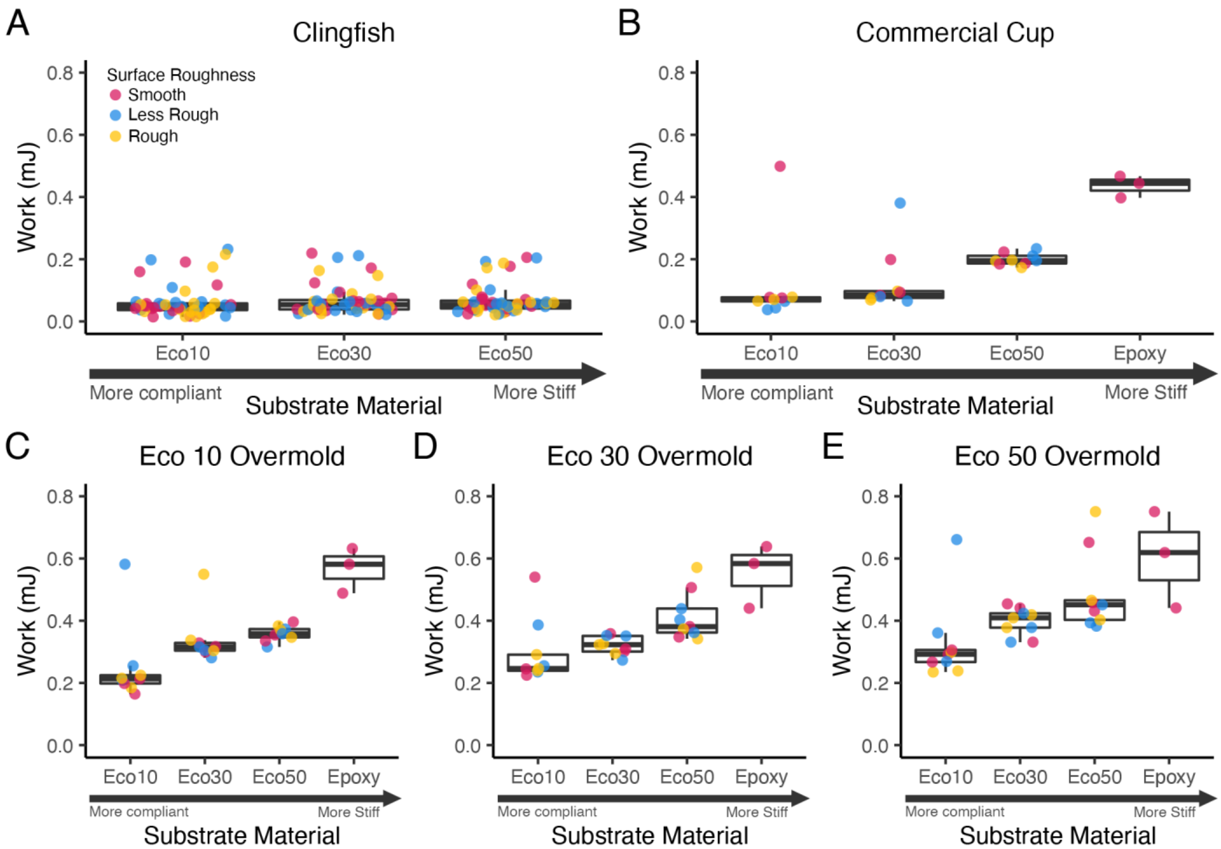

Figure 4. The amount of work (mJ) required to pull off A) the Northern clingfish, B) commercial suction cups, and C-D) the different overmold suction cups from substrates of varying compliance and surface roughness. Boxplots show the median, upper and lower quartiles, and interquartile range. Dots are individual observations colored by the surface roughness (Magenta = Smooth (0 µm), Blue = Less Rough (59 µm), and Yellow = Rough (269 µm)), to indicate that surface roughness had little or no effect on work for any cup type.

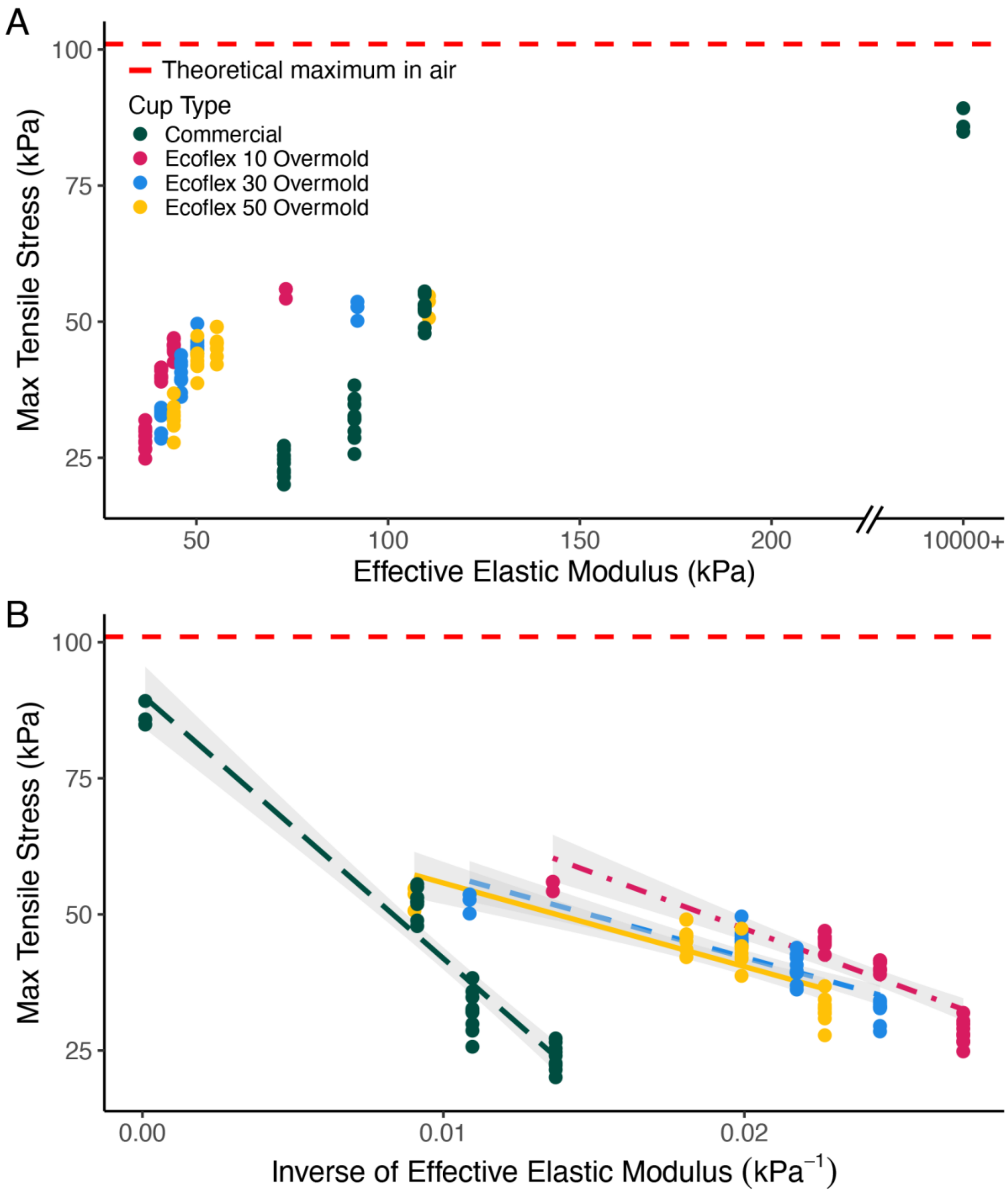

Figure 5. Scatterplots showing the relationship between the maximum tensile stress and effective elastic modulus (A) and the inverse of effective elastic modulus (B) for all of the man-made suction cups on both smooth and rough substrates. The relationship between stress and effective elastic modulus is nonlinear; note the break in the x-axis. However, the relationship between in stress and the inverse of the modulus was best described by a model that fit separate regression lines for each suction cup type (see Results). Colored dots and lines represent the different man-made cups (Green = Commercial Cup, Magenta = Ecoflex 10 Overmold, Blue = Ecoflex 30 Overmold, and Yellow = Ecoflex 50 Overmold). Gray bands represent 95% confidence intervals. The red dotted line indicates the theoretical stress maximum in air (101 kPa).

Table 1. Comparison of peak stress (kPa) for the Northern clingfish, commercial suction cup, and three overmold cup variants on 10 substrates that varied in their material stiffness and surface roughness.

	Clingfish		**Commercial**		**Ecoflex 10**		**Ecoflex 30**		**Ecoflex 50**	
	FE ± s.e.	CI	FE ± s.e.	CI	FE ± s.e.	CI	FE ± s.e.	CI	FE ± s.e.	CI
Compliant (Ecoflex 10)										
Smooth	19.0 ± 1.41	16.2, 21.9	24.7 ± 1.44	21.7, 27.7	28.9 ± 0.91	27.0, 30.9	33.2 ± 1.07	30.9, 35.4	33.5 ± 1.12	31.2, 35.9
Less Rough	23.0 ± 1.41	20.2, 25.9	21.4 ± 1.44	18.4, 24.4	28.9 ± 0.91	27.0, 30.8	31.9 ± 1.07	39.6, 34.1	33.8 ± 1.12	31.4, 36.1
Rough	20.0 ± 1.41	17.2, 22.8	25.3 ± 1.44	22.3, 28.3	27.2 ± 0.91	25.3, 29.1	32.0 ± 1.07	29.8, 34.3	30.2 ± 1.12	27.9, 32.5
Less stiff (Ecoflex 30)										
Smooth	30.0 ± 1.41	27.2, 32.8	35.5 ± 1.44	32.5, 38.5	40.4 ± 0.91	38.4, 42.3	37.5 ± 1.07	35.2, 39.7	41.2 ± 1.12	38.9, 43.6
Less Rough	29.4 ± 1.41	26.6, 32.2	28.8 ± 1.44	25.8, 31.8	40.1 ± 0.91	38.1, 42.0	40.5 ± 1.07	38.2, 42.7	43.2 ± 1.12	40.9, 45.6
Rough	28.9 ± 1.41	26.1, 31.7	32.4 ± 1.44	29.4, 35.4	41.3 ± 0.91	39.4, 43.3	42.2 ± 1.07	40.0, 44.4	45.1 ± 1.12	42.8, 47.5
Stiff (Ecoflex 50)										
Smooth	35.4 ± 1.41	32.6, 38.2	51.9 ± 1.44	48.9, 54.9	46.0 ± 0.91	44.1, 47.9	46.7 ± 1.07	44.5, 49.0	46.8 ± 1.12	44.5, 49.1
Less Rough	33.1 ± 1.41	30.2, 35.9	53.3 ± 1.44	50.3, 56.3	44.4 ± 0.91	42.5, 46.3	45.1 ± 1.07	42.8, 47.3	43.9 ± 1.12	41.6, 49.1
Rough	33.2 ± 1.41	30.4, 36.0	51.4 ± 1.44	48.4, 54.4	45.7 ± 0.91	43.8, 47.7	45.4 ± 1.07	43.1, 47.6	47.1 ± 1.12	44.8, 49.4
Hard (Epoxy)										
Smooth	33.2 ± 1.02	31.2, 35.3	86.6 ± 1.44	83.6, 89.6	55.4 ± 0.907	53.5, 57.3	52.2 ± 1.07	49.9, 54.4	53.0 ± 1.12	50.7, 55.4
Goodness-of-fit	$R^2_{LMM(m)}$	$R^2_{LMM(c)}$	$R^2_{LMM(m)}$	$R^2_{LMM(c)}$	$R^2_{LMM(m)}$	$R^2_{LMM(c)}$	$R^2_{LMM(m)}$	$R^2_{LMM(c)}$	$R^2_{LMM(m)}$	$R^2_{LMM(c)}$
(Nagakawa's R^2)	0.473	0.878	0.984	NA	0.969	0.973	0.928	NA	0.927	NA

A separate statistical analysis was performed for each cup type based on the model: lmer(Stress ~ Substrate stiffness * Surface roughness + (1|Individual)). The fixed effects (FE), standard error, and 95% confidence intervals (CI) were estimated with the *emmeans* R package. Nagakawa's R^2 values were calculated using the *performance* R package. $R^2_{LMM(m)}$ represents the variance explained by only the fixed effects; whereas, $R^2_{LMM(c)}$ represents the variance explained by the fixed and random effects. NA $R^2_{LMM(c)}$ values indicate that the random effect explained zero variance.

Table 2. Comparison of attachment time (s) for the Northern clingfish, commercial suction cup, and three overmold cup variants on 10 substrates that varied in their material stiffness and surface roughness.

	Clingfish		**Commercial**		**Ecoflex 10**		**Ecoflex 30**		**Ecoflex 50**	
	FE ± s.e.	CI	FE ± s.e.	CI	FE ± s.e.	CI	FE ± s.e.	CI	FE ± s.e.	CI
Compliant (Ecoflex 10)										
Smooth	0.99 ± 0.05	0.90, 1.09	0.90 ± 0.15	0.53, 1.26	0.89 ± 0.16	0.55, 1.23	0.93 ± 0.14	0.58, 1.27	1.23 ± 0.21	0.64, 1.82
Less Rough	0.98 ± 0.05	0.89, 1.08	0.53 ± 0.15	0.16, 0.89	1.24 ± 0.16	0.90, 1.58	1.23 ± 0.14	0.89, 1.57	1.70 ± 0.21	1.12, 2.29
Rough	0.90 ± 0.05	0.80, 0.10	0.65 ± 0.15	0.28, 1.01	0.93 ± 0.16	0.59, 1.27	1.16 ± 0.14	0.81, 1.50	1.20 ± 0.21	0.62, 1.79
Less stiff (Ecoflex 30)										
Smooth	0.94 ± 0.05	0.84, 1.03	0.79 ± 0.15	0.43, 1.16	1.03 ± 0.16	0.69, 1.37	1.23 ± 0.14	0.89, 1.58	1.42 ± 0.21	0.83, 2.00
Less Rough	0.84 ± 0.05	0.74, 0.93	0.76 ± 0.15	0.40, 1.13	1.01 ± 0.16	0.67, 1.35	1.26 ± 0.14	0.91, 1.60	1.27 ± 0.21	0.69, 1.86
Rough	0.84 ± 0.05	0.74, 0.93	0.64 ± 0.15	0.27, 1.00	1.36 ± 0.16	1.02, 1.70	1.08 ± 0.14	0.73, 1.42	1.30 ± 0.21	0.71, 1.88
Stiff (Ecoflex 50)										
Smooth	0.83 ± 0.05	0.74, 0.93	0.88 ± 0.15	0.51, 1.24	1.08 ± 0.16	0.74, 1.42	1.30 ± 0.14	0.95, 1.64	1.28 ± 0.21	0.70, 1.87
Less Rough	0.82 ± 0.05	0.72, 0.92	0.99 ± 0.15	0.62, 1.36	1.05 ± 0.16	0.71, 1.39	1.31 ± 0.14	0.97, 1.66	1.32 ± 0.21	0.74, 1.91
Rough	0.80 ± 0.05	0.71, 0.90	0.87 ± 0.15	0.50, 1.24	1.08 ± 0.16	0.74, 1.42	1.11 ± 0.14	0.77, 1.45	1.45 ± 0.21	0.86, 2.04
Hard (Epoxy)										
Smooth	-	-	1.15 ± 0.15	0.78, 1.51	1.67 ± 0.16	1.33, 2.01	1.07 ± 0.14	0.72, 1.41	1.69 ± 0.21	1.10, 2.28
Goodness-of-fit	$R^2_{LMM(m)}$	$R^2_{LMM(c)}$	$R^2_{LMM(m)}$	$R^2_{LMM(c)}$	$R^2_{LMM(m)}$	$R^2_{LMM(c)}$	$R^2_{LMM(m)}$	$R^2_{LMM(c)}$	$R^2_{LMM(m)}$	$R^2_{LMM(c)}$
(Nagakawa's R^2)	0.117	0.903	0.321	0.678	0.387	0.452	0.19	0.615	0.186	0.736

A separate statistical analysis was performed for each cup type based on the model: lmer(Time ~ Substrate stiffness * Surface roughness + (1|Individual)). The fixed effects (FE), standard error, and 95% confidence intervals (CI) were estimated with the *emmeans* R package. Nagakawa's R^2 values were calculated using the *performance* R package. $R^2_{LMM(m)}$ represents the variance explained by only the fixed effects; whereas, $R^2_{LMM(c)}$ represents the variance explained by the fixed and random effects.

Table 3. Comparison of the work (mJ) required to remove the Northern clingfish, commercial suction cup, and three overmold cup variants from 10 substrates that varied in their material stiffness and surface roughness. The clingfish values were size-corrected relative to disc area (see Methods).

	Clingfish		**Commercial**		**Ecoflex 10**		**Ecoflex 30**		**Ecoflex 50**	
	FE ± s.e.	CI	FE ± s.e.	CI	FE ± s.e.	CI	FE ± s.e.	CI	FE ± s.e.	CI
Compliant (Ecoflex 10)										
Smooth	0.06 ± 0.01	0.04, 0.09	0.22 ± 0.06	0.10, 0.336	0.19 ± 0.05	0.09, 0.29	0.34 ± 0.05	0.23, 0.44	0.29 ± 0.07	0.15, 0.42
Less Rough	0.07 ± 0.01	0.05, 0.10	0.05 ± 0.06	-0.07, 0.168	0.35 ± 0.05	0.25, 0.45	0.29 ± 0.05	0.19, 0.40	0.43 ± 0.07	0.30, 0.57
Rough	0.06 ± 0.01	0.03, 0.09	0.07 ± 0.06	-0.05, 0.191	0.21 ± 0.05	0.11, 0.31	0.26 ± 0.05	0.15, 0.36	0.26 ± 0.07	0.12, 0.39
Less stiff (Ecoflex 30)										
Smooth	0.08 ± 0.01	0.05, 0.10	0.13 ± 0.06	0.01, 0.25	0.32 ± 0.05	0.22, 0.41	0.32 ± 0.05	0.22, 0.43	0.41 ± 0.07	0.27, 0.54
Less Rough	0.07 ± 0.01	0.04, 0.09	0.18 ± 0.06	0.06, 0.29	0.30 ± 0.05	0.20, 0.40	0.33 ± 0.05	0.22, 0.43	0.38 ± 0.07	0.24, 0.51
Rough	0.06 ± 0.01	0.03, 0.09	0.08 ± 0.06	-0.04, 0.20	0.40 ± 0.05	0.30, 0.50	0.32 ± 0.05	0.21, 0.42	0.40 ± 0.07	0.27, 0.54
Stiff (Ecoflex 50)										
Smooth	0.07 ± 0.01	0.05, 0.10	0.20 ± 0.06	0.08, 0.32	0.36 ± 0.05	0.26, 0.46	0.41 ± 0.05	0.31, 0.52	0.51 ± 0.07	0.38, 0.65
Less Rough	0.07 ± 0.01	0.04, 0.09	0.21 ± 0.06	0.09, 0.33	0.35 ± 0.05	0.25, 0.45	0.40 ± 0.05	0.30, 0.51	0.41 ± 0.07	0.27, 0.54
Rough	0.07 ± 0.01	0.04, 0.09	0.19 ± 0.06	0.07, 0.31	0.37 ± 0.05	0.27, 0.47	0.43 ± 0.05	0.32, 0.53	0.54 ± 0.07	0.41, 0.67
Hard (Epoxy)										
Smooth	-	-	0.44 ± 0.06	0.32, 0.56	0.57 ± 0.05	0.47, 0.67	0.55 ± 0.05	0.45, 0.66	0.60 ± 0.07	0.47, 0.74
Goodness-of-fit	$R^2_{LMM(m)}$	$R^2_{LMM(c)}$	$R^2_{LMM(m)}$	$R^2_{LMM(c)}$	$R^2_{LMM(m)}$	$R^2_{LMM(c)}$	$R^2_{LMM(m)}$	$R^2_{LMM(c)}$	$R^2_{LMM(m)}$	$R^2_{LMM(c)}$
(Nagakawa's R^2)	0.010	0.958	0.538	NA	0.597	NA	0.474	NA	0.46	NA

A separate statistical analysis was performed for each cup type based on the model: lmer(Work ~ Substrate stiffness * Surface roughness + (1|Individual)). The fixed effects (FE), standard error, and 95% confidence intervals (CI) were estimated with the *emmeans* R package. Nagakawa's R^2 values were calculated using the *performance* R package. $R^2_{LMM(m)}$ represents the variance explained by only the fixed effects; whereas, $R^2_{LMM(c)}$ represents the variance explained by the fixed and random effects. NA $R^2_{LMM(c)}$ values indicate that the random effect explained zero variance.

Table S1. Morphometric and performance data for the clingfish, commercial suction cups, and overmold suction cups.

Click here to download Table S1

Table S2. Load extension curve data for the best clingfish, commercial, and overmold suction cup trails.

Click here to download Table S2

R script file containing the code used to perform the analyses and plot the figures used in this study.R script file containing the code used to perform the analyses and plot the figures used in this study.

Click here to download Dataset 1